UvA-DARE (Digital Academic Repository)

Novel, Moon and Mars, partial gravity simulation paradigms and their effects on the balance between cell growth and cell proliferation during early plant development

Manzano, A.; Herranz, R.; den Toom, L.A.; te Slaa, S.; Borst, G.; Visser, M.; Medina, F.J.; van Loon, J.J.W.A.

[Link to publication](#)

1   **Supplementary Information**

2

3   **Background of the Software RPM**

4   The RPM is a mechanism that consist of two perpendicular axed frames driven by motors that

5   continually rotate an experiment frame relative to the world frame (Figures 1 and S1). Or since

6   the gravity direction is fixed in the world frame, it continually rotates the gravity direction

7   relative to the experimental frame ergo the sample. The gravity vector acceleration can be

8   averaged over time resulting in a certain mean gravity ranging from the theoretical 0 g to 1 g

9   where 1 g is the Earth gravity acceleration of 9.81 m/s^2. If the mean gravity is close to 0 g this is

10   called zero gravity or better microgravity, in order to take into account small deviations such as

11   distance from the center of rotation (see e.g. [1,2]). If the mean gravity is between 0 and 1 g it is

12   referred to as partial gravity or hypo-gravity. Note that the experiment must be placed in the

13   center of the experimental frames to prevent it from being exposed to possibly significant

14   centrifugal acceleration [1,3].

15
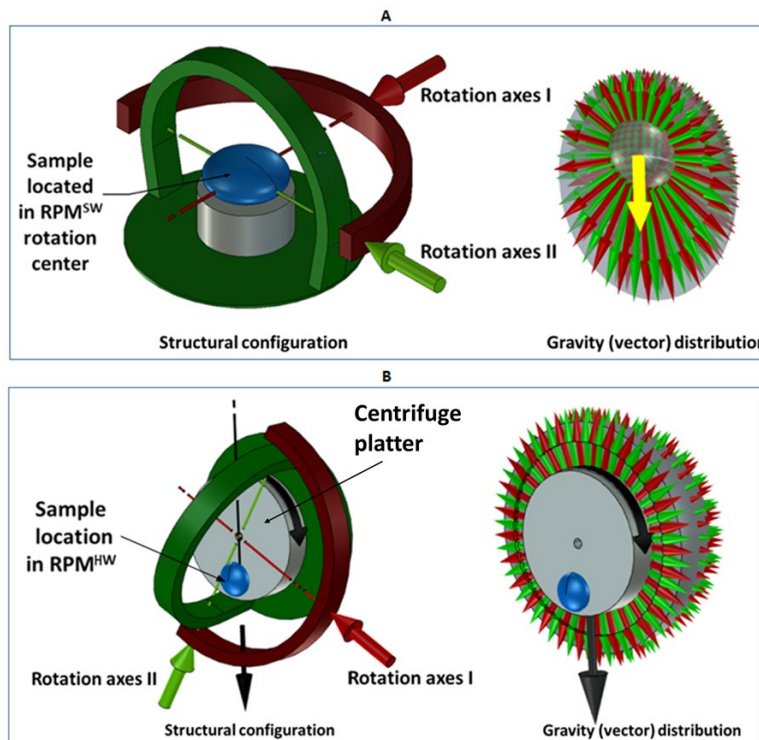
16
17   *Figure S1: Set up of partial g simulation systems. A: Cartoon of the software directed simulated partial*

18   *gravity Random Positioning Machine (RPM^{SW}). Left the hardware / axes configuration. Right: Software*

19   *directing the motion of this RPM can be set to have a certain degree of preference along the Earth gravity*

20 *vector. Resultant g represented by yellow arrow. B: The hardware directed simulated partial gravity*
21 *RPM (RPM^{HW}). Left the hardware configuration consisting of a regular (large size) RPM where the*
22 *partial g is generated by a centrifuge (grey). Right the resultant g-load depicted by the black arrow*
23 *pointing from the rotation axis of the centrifuge outwards.*
24
25 **Kinematics**
26 The joint space of the mechanism is the set of motor angles (q1, q2) and forms a 2-plane. The
27 task space is the set of gravity directions relative to the experiment and forms a sphere (Figure
28 S2A). The sphere is embedded in 3-space and can be parametrized by the three components of
29 the gravity vector (g1, g2, g3). The function from the motor angles to the gravity direction is
30 called the forward kinematics and is given by:

$$gravity(t) = forward\ (q) = \begin{bmatrix} cos(q_1)cos(q_2) \\ cos(q_1)sin(q_2) \\ sin(q_1) \end{bmatrix}$$

31
32 where the motor angles can be identified with the latitude and longitude of a sphere. The inverse
33 function from the gravity direction to the motor angles is called the inverse kinematics.
34
35 The motor angles follow a defined path in joint space q(t) that results in a certain gravity
36 direction path in task space g(t). The goal is to set a motor path q(t) such that the gravity path g(t)
37 has the desirable properties. In the following two such desirable properties for g(t) will be
38 proposed and one algorithm for choosing a motor path q(t) that has these properties. First they
39 will be discussed in the context of microgravity and later they will be generalized to partial
40 gravity.
41
42 **Zero mean**
43 The gravity vector g(t) can be averaged over time resulting in a certain mean gravity:
44

$$mean(gravity(t)) = \frac{1}{t} \int gravity(t)dt$$

45
46 The first and most obvious desirable property is that the mean converges to zero or (0, 0, 0).
47 Most algorithms from literature have this property [4,5]. For example also a simple clinostat has it.
48 However, for some samples this may not be sufficient. Note that the rate of convergence must be
49 fast compared to the relevant time constants of the experiment. For example the perception time

50 for plants is in the order of seconds [6], for the single cell organism *Euglena gracilis*, a similar time

51 order of around five seconds has been reported [7].

52

53 **Uniform distribution**

54 The space of al gravity directions provides a sphere. The gravity path g(t) walks over this sphere

55 and visits different points. The relative times that it spends in the neighborhoods of different

56 points result in a certain distribution over the sphere. If the path visits all points equally the path

57 converges to a uniform distribution (Figure S2A), and if it visits some points more than others

58 the path converges to a non-uniform distribution. A simple 2D clinostat for example only visits 1

59 great circle on the sphere (which can be identified with the equator of the sphere), and therefore

60 results in a very non-uniform distribution. Different distributions can result in same mean

61 gravity. For example both the uniform distribution and the clinostat distribution result in the

62 same zero mean.

63 Certain experiments may be more sensitive to gravity in some directions than in other directions,

64 and are therefore sensitive to the distribution of the gravity vector. Such experiments would

65 result in different outcomes for different distributions. Note that such experiments are also

66 sensitive to how the experiment is fixed in the experiment frame because the distribution is

67 relative to the experiment frame.

68 The only distribution that has no bias in certain directions is the uniform distribution. Therefore

69 the second desirable property of a gravity path is that the distribution converges to a uniform

70 distribution. Note that also here the rate of convergence must preferably be less compared to the

71 relative time constants of the experiment.

72 A good measure for the uniformity is the standard deviation of the density of the distribution

73 over surface of the sphere. Here density (t, q) is the amount of time the gravity direction has

74 spent in a neighborhood of f(q).

$$standard\ deviation\big(density(q,t)\big) = \sqrt{\frac{1}{4\pi t} \iint \left(density(q,t) - \frac{t}{4\pi}\right)^2 \cos(q_1)dq_1q_2}$$

75

76 Most algorithms from literature (for example figure 4 of Wuest *et al.*[4]) including the algorithm

77 for the first generation of the RPM [2] result in a uniform distribution in the latitude – longitude

78 plane. However, when this plane is folded around the sphere the density at the poles becomes

79 much higher than at the equator. This is similar to a globe where the density of meridians at the

80   poles is higher than at the equator. Although the first property (zero mean) is met, the second

81   property (uniform distribution) is not met.

82

83   **Random walk**

84   The gravity path that is proposed consists of a random walk over the surface of the sphere. The

85   random walk consists of a sequence of steps and turns. The steps are geodesic curves of a certain

86   length which on the surface of a sphere correspond to pieces of great circles. The turns are

87   uniformly distributed between plus or minus a defined maximum angle. It can be proven that

88   such a random walk converges to a uniform distribution over the sphere [8].

89
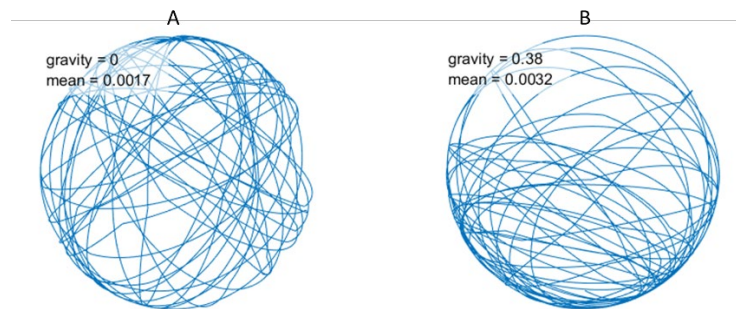
90

91   *Figure S2: The beginning of a path of the gravity vector over the sphere for zero gravity (on the left) and*

92   *for Mars (on the right). It can be seen that on the left the trajectory is distributed uniformly over the*

93   *sphere, while on the right it trajectory spends more time at the bottom than at the top, resulting in a*

94   *partial gravity factor of 0.38. Mean in the figure is the mean error between the desired and the actual*

95   *partial gravity factor after running for 1 hour.*

96

97   **Generalization to partial gravity**

98   The algorithm for zero gravity (random walk over a sphere) can be generalized to partial gravity

99   by introducing a prolate spheroid. A prolate spheroid is an ellipse that is rotated around its major

100   axis and has the shape of a rugby ball (see Figures 1B and S3). It has two focal points. One of the

101   focal points is fixed in the center of the sphere of gravity directions, and the other focal point is

102   moved in the direction of the desired partial gravity. Now instead of performing a random walk

103   over the sphere a geodesic random walk over the spheroid is performed. The resulting random

104   walk will converge to a uniform distribution over the spheroid. The proof from [8] still holds and

105   this random walk is then projected from the spheroid onto the sphere.

106   Because a relatively large part of the surface of the spheroid is on one side of the sphere and a

107   relatively small part on the other side (Figure S2B), the gravity direction spends more time on

108   that side of the sphere. So if the gravity vector is averaged over time, it converges to a certain

109   non-zero partial gravity. By varying the ellipticity of the spheroid from 0 to 1 the simulated

110   partial gravity is varied from 0 to 1.

111   The two desirable properties can be generalized to partial gravity as follows. For the first

112   property (zero mean) instead of looking at the norm of the mean gravity we look at the norm of

113   the difference between the mean gravity and the desired partial gravity. For the second property

114   (uniform density), instead of looking at the standard deviation of the density of the distribution

115   over the sphere, we look at the distribution over the spheroid.

116
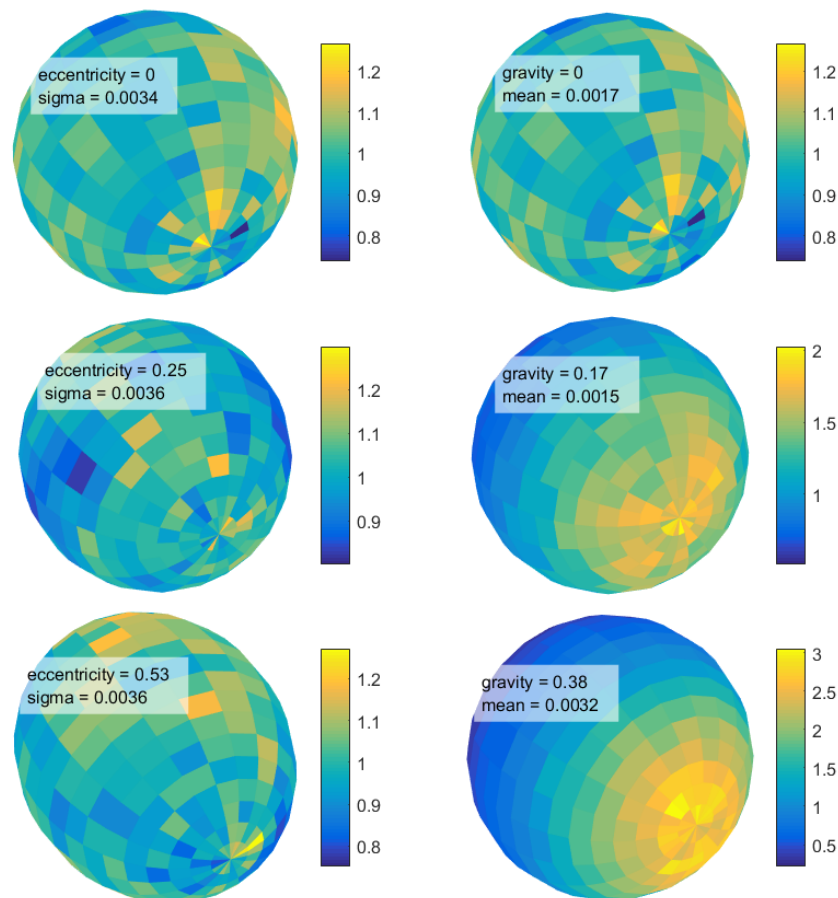
117
118   *Figure S3: Distribution of the path over a spheroid (on the left) and resulting distribution of the gravity*

119   *vector over the sphere (on the right) after running for 1 hour. The top row is for zero gravity (eccentricity*

120   *of 0), the middle row for the Moon (eccentricity of 0.25 resulting in partial gravity of 0.17) and the*

121   *bottom row for Mars (eccentricity of 0.53 resulting in a partial gravity of 0.38). The scale bars represent*

122   *the normalized density where 1 is uniform density. One wants the pictures on the left to be as uniform as*

123   *possible. For the pictures on the right it depends on the desired partial gravity factor. Mean is the mean*

124   *error between the desired and the actual partial gravity factor. Sigma is the standard deviation of the*

125   *normalized density of the distribution relative to a uniform distribution.*

126

References

128 1 van Loon, J. J. W. A. (2007). Some history and use of the Random Positioning Machine, RPM, in gravity
129   related research. Adv Space Res 39, 1161-5.

130 2 Borst, A. G., van Loon, J. J. W. A. (2009). Technology and developments for the random positioning
131   machine, RPM. *Microgravity Sci. Technol* **21**, 6.

132 3 Hasenstein, K. H., and van Loon, J. J. W. A. (2015). Clinostats and other rotating systems — Design,
133   function, and limitations. in "Generation and Applications of Extra-Terrestrial Environments on
134   Earth", D.A. Beysens & J.J.W. A. van Loon (eds.). *River Publishers, Denmark.*

135 4 Wuest S.L., Richard S., Walther I., R Furrer R., Anderegg R., Sekler J., Egli M. (2014) A novel
136   microgravity simulator applicable for three dimensional cell culturing. Microgravity Science and
137   Technology, **26(2)**, 77 – 88.

138 5 Kim Y.J., Jeong A.J., Kim M., Lee C., Ye S.K., Kim S. (2017) Time-averaged simulated microgravity
139   (taSMG) inhibits proliferation of lymphoma cells, L-540 and HDLM-2, using a 3D clinostat. Biomed
140   Eng Online. **16:48**, 1-12.

141 6 Perbal G., Jeune B., Lefranc A., Carnero-Diaz E., Driss-Ecole D. (2002) The dose–response curve of the
142   gravitropic reaction: a re-analysis. Physiol Plant. **114(3)**, 336-342.

143 7 Lebert M., Porst M., Richter P, Hader D.P. (1999) Physical characterization of gravitaxis in Euglena
144   gracilis. J Plant Physiol. **155(3)**, 338-343.

145 8 Jørgensen E. (1975) The central limit problem for geodesic random walks. Zeitschrift für
146   Warscheinlichkeitstheorie und Verwandte Gebiete. **32(1)**, 1 – 64.